Journal of the Society of Automotive Engineers Malaysia
Volume 2, Issue 1, pp 43-59, January 2018
e-ISSN 2550-2239

Vehicle Localization Using Wheel Speed Sensor (WSS) and Inertial Measurement Unit (IMU)

W. M. H. Wan Azree[1], M. A. Abdul Rahman[*2] and H. Zamzuri[3]

[1]Vehicle System Engineering (VSE), Malaysia-Japan International Institute of Technology, Universiti Teknologi Malaysia, Jalan Sultan Yahya Petra, 54100 Kuala Lumpur, Malaysia
[2]Department of Electronic System Engineering, Malaysia-Japan International Institute of Technology, Universiti Teknologi Malaysia, Sultan Yahya Petra, 54100 Kuala Lumpur, Malaysia

[*]*Corresponding author: azizi.kl@utm.my*

ORIGINAL ARTICLE **Open Access**

Article History:

Received
26 Apr 2017

Received in revised form
1 Nov 2017

Accepted
8 Dec 2017

Available online
1 Jan 2018

Abstract – *The advent of autonomous driving has led researchers toward a whole new technological age where vehicle positioning and localization system form the back bone of an autonomous electric vehicle. However, localization becomes poor as a vehicle enters GPS-denied areas due to multi path errors. Autonomous vehicle, in addition, needs to be localized from time to time and be guided on the right path along its destination. The purpose of this study is to overcome the problem of adopting an alternative method by using the vehicle's Wheel Speed Sensor (WSS) for localization. WSS as an auxiliary sensor is attached to the vehicle's wheel to track its position upon considering its travelling speed in a period of time. This is done in such a way that the existence of obscured portion along the guideway will be neglected. The data obtained from WSS are combined with yaw rate from an Inertial Measurement Unit (IMU) through Kinematic Modelling algorithm and then be converted to get the local position coordinates. In order to analyse whether the yaw rate produced by IMU is acceptable or not, comparison with simulation is needed. A Bicycle Model is used to generate simulated yaw rate from the steering angle of the vehicle and Kalman Filter estimates the simulated yaw rate to be close with the raw yaw rate. Therefore, this will clarify that the yaw rate obtained from IMU is acceptable and that true localization path is generated.*

Keywords: Autonomous vehicle, vehicle localization, global positioning system, wheel speed sensor, inertial measurement unit, bicycle model, Kinematic modelling, Kalman filter

Journal homepage: www.journal.saemalaysia.org.my

1.0 INTRODUCTION

In this age of globalization, millions of drivers ply the road on a daily basis. According to the 2015 World Bank Report, the population of Kuala Lumpur spends up to 500 million hours a

year stuck in traffic, while burning up to 1.2 billion litres of fuel (about 315 million gallons). Such a situation, which occurs due to the vast number of vehicles entering the city at the same time, results in losses estimated to exceed 2 per cent of the country's Gross Domestic Product.

Accidents along the guideway will often make the situation worse. According to an article on the Internet, around 10 per cent of workers are caught in gridlocks in Malaysia on a daily basis culminating in a loss of productivity amounting to RM5.51 billion a year (Says.com, 2015; Tash, 2016). In addition, drivers often become exhausted and this will also affect their productivity at work. Perhaps development of autonomous vehicle can offer a solution to these drivers.

Localization plays an important role to automate a vehicle, thus leading to auto-pilot driving on the motorway. It guides a vehicle to move from one point to another. The Global Positioning System (GPS) is used to locate the vehicle upon receiving signal pertaining to its position from satellites. However, the vehicle has to be in the range of orbiting satellite. When the vehicle enters urban areas, some portions are obstructed by trees, underground tunnels, basement areas as well as high rise buildings. Such a scenario leads to a multi path error, thus resulting in inaccurate positioning data from the GPS, as explained in Figure 1.

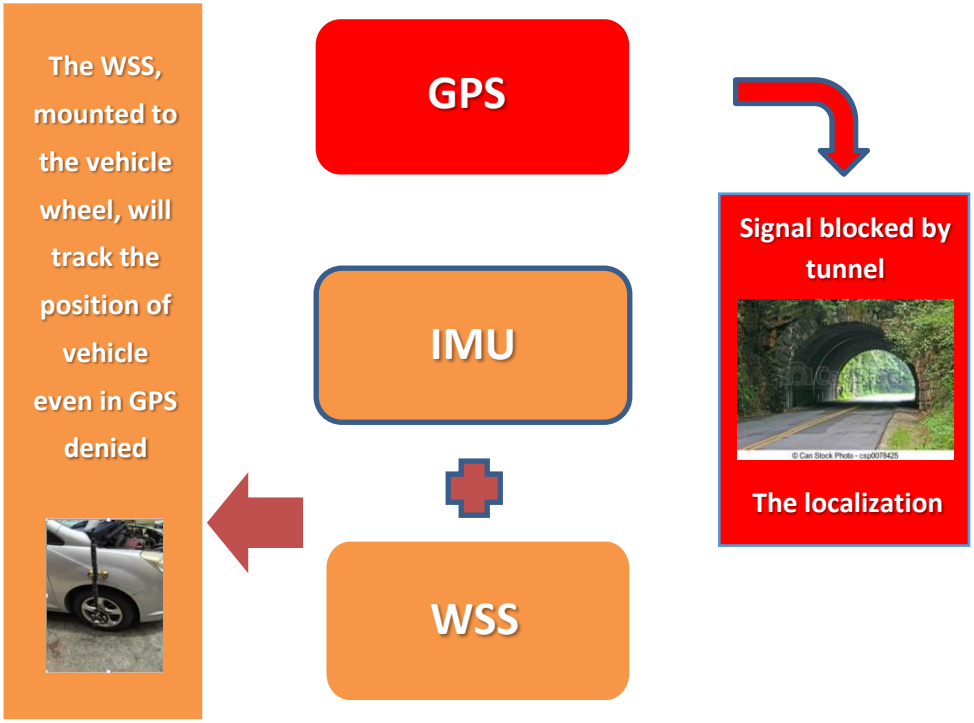

Figure 1: Overview of the study

As shown in Figure 2, a multi-path error occurs when signals from GPS satellite bounce off buildings, as the GPS receiver gets confused by the extra time the signal took to reach it. Hence, sudden large errors in position can be observed. The WSS offers a practical alternative to overcome data inaccuracy for localization purposes. According to Axelrad et al. (1996), multipath reflections affect both the carrier phase measured by the receiver and Signal-to-Noise Ratio (SNR).

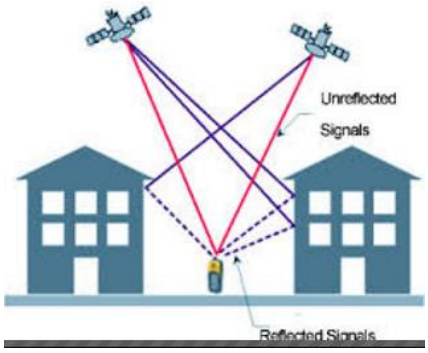

Figure 2: Occurrence of multi-path error

The WSS records the travelling speed of a vehicle within a period of time. Although the ECU has the capability to perform the same task, its accuracy is arguable. A probable reason for this is that ECU is not specialized to control vehicle speed per se but has to handle a multitude of sensors within the engine operations, interpreting them and adjusting the actuator. Figure 3 shows the operations controlled by the ECU.

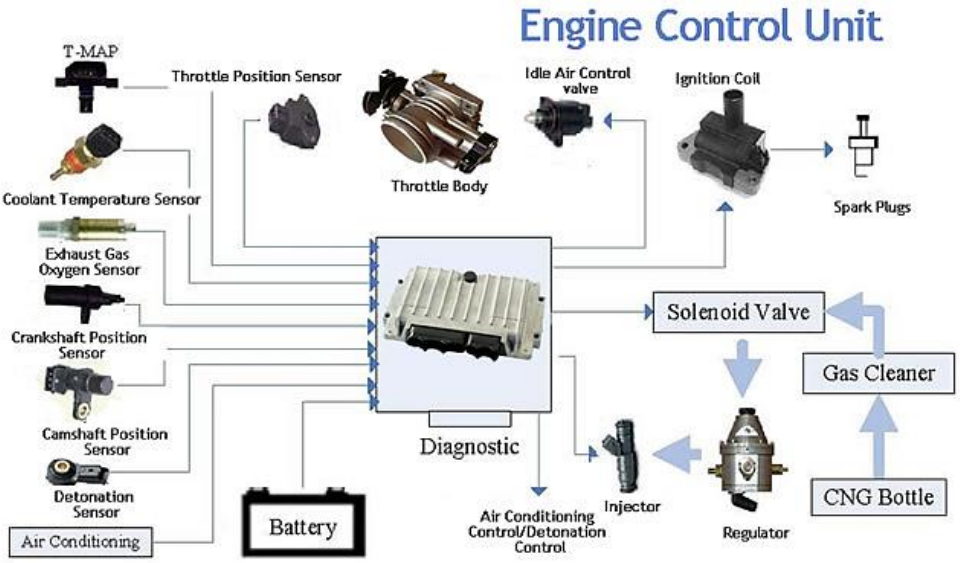

Figure 3: Engine Control Unit operations (AerMech.com, 2014)

1.1 Fundamentals of Mobile Vehicle Localization

An autonomous operation resembles that of a practical mobile robot, albeit in smaller scale. Although robotic technology has been around for many years, its application is now able to be successfully integrated into autonomous vehicle operations. According to Belta and Kumar (2001), in order for a robot to be autonomously navigated, it must be capable of localizing itself.

Fundamental calculation of localization algorithm starts with a model of the sensor and a model of the vehicle utilized for restriction. The vehicle display depicts how it moves when we apply diverse control activities, and structures the premise on which vehicle area assessments are made. Figure 4 demonstrates a straightforward model of a vehicle.

The vector [x (k), y (k), ø (k)] signifies both vehicle position and its orientation within a discrete time of k. The vehicle moves by guiding a solitary front wheel through a point g(k) and by driving the same wheel to accomplish forward speed V(k). Amid a period interim T, displacement of the vehicle position from an area [x(k-1),y(k-1),ø(k-1)] at time k-1, to an area [x(k),y(k),ø(k)], at time k and a forward speed. V (k). Marino et al. (2012) in their article "Integrated driver and active steering control for vision-based lane keeping" reported that a simple geometry can be shown if everything is known perfectly, hence the new location can be written in terms of the old location and these control parameters are as follows:

$$\begin{pmatrix} x(k) \\ y(k) \\ \emptyset(k) \end{pmatrix} = \begin{pmatrix} x(k-1) + \Delta TV(k)\cos(\emptyset(k-1) + g(k)) \\ y(k-1) + \Delta TV(k)\sin(\emptyset(k-1) + g(k)) \\ \emptyset(k-1) + (V(k)/B)\sin(g(k)) \end{pmatrix} \quad (1)$$

Where B is the distance from the rear axle to the centre of steer. On a basic level, when in the event that we know all the control and drive inputs, then we can foresee precisely where the vehicle will be anytime later.

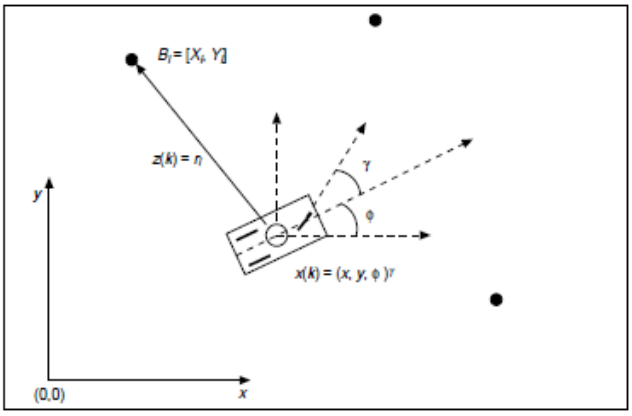

Figure 4: A straightforward model of a vehicle with fixed beacons placed

1.2 Kalman Filter

Kalman Filter is basically an arrangement of scientific conditions that ideally execute predictor-corrector sort estimator as in it limits the evaluated mistake covariance when some assumed conditions are met" (Welch & Bishop, 2006).

The KF addresses the general issue of attempting to evaluate the state x n of a discrete-time controlled process represented by the direct stochastic distinction condition as of the accompanying:

$$xk = Axk - 1 + Buk + wk - 1 , \quad (2)$$

with an estimation z ∈ ℜm that is:

$$zk = Hxk + vk . \quad (3)$$

The random factors wk and vk speak to the procedure and measurement noise (individually). They are thought to be autonomous, white and with typical likelihood appropriations:

$$p\, w(\,) \sim N(0, Q)\,, \tag{4}$$

$$p\, v(\,) \sim N(0, R)\,. \tag{5}$$

Practically speaking, the procedure noise covariance Q and measurement noise covariance R grids may change with each time step or estimation, as it is we may accept they are consistent. Likewise, the n × n matrix of variable, A in Equation 2 relates to the state in the past time step k – 1 to the state at the present stride, without either a driving capacity or process noise. Do take note that, variable A might change with each time step, although here we expect it to be steady.

The n × l matrix B relates to the discretionary control input u ∈ ℜl to the state x. The m × n matrix of variable H in the Equation 3 relates to the state to the estimation zk. Practically speaking, variable H may change with each time step or estimation, although here, we accept it to be consistent.

1.3 Bicycle Model

Bicycle model is a function widely used in research to resemble the parameter of a real vehicle for simulation purposes. According to Taheri (1990), there are seven main parameters in total that are demanded to form the bicycle model's state-space, namely the look ahead distance, cornering stiffness of front tires, cornering stiffness of rear tires, distance of centre of gravity from front axle, distance of centre of gravity from rear axle, vehicle total mass and the vertical axle inertia. Moreover, the bicycle model will take into account every detail of the vehicle parameter to generate yaw rate, as shown in Figure 5.

The Bicycle model will produce four main outputs which include the lateral velocity, lateral offset, heading offset and the yaw rate. As for this research, only the yaw rate will be used.

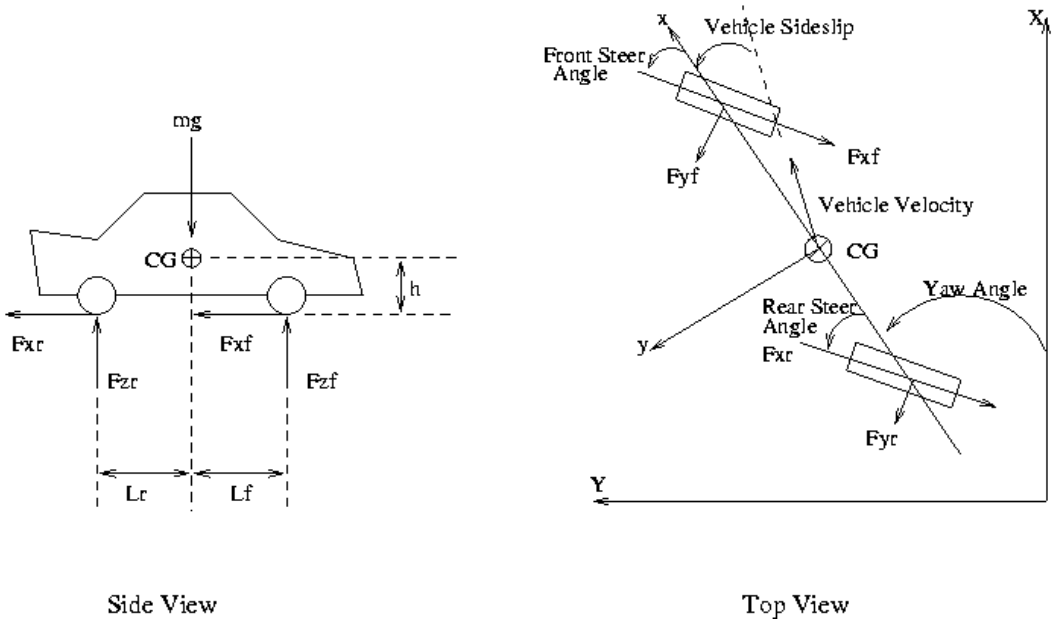

Figure 5: Free body diagram of the vehicle

2.0 METHODOLOGY

2.1 Research Setup

There are three main instruments necessary in this research: the GPS, WSS and IMU. All these instruments will be installed to the experimental vehicle, which is a seven seater Proton Exora 1.6 cc. The reason for using a seven-seater vehicle instead of a sedan or compact car is because it is the only vehicle available for this research. The vehicle is provided by car manufacturer Perusahaan Otomobil Nasional (PROTON) to VSE laboratory (ikohza) for research purposes (Figure 6).

Figure 6: The test bed instrumented vehicle (i-Drive)

The GPS used in this study is known as MINITAUR Box (Figure 7). Its speed measurement accuracy can be better than 0.1 km/h and its output updated rate for the speed can vary from 1 Hz to 100 Hz with no distance limit. Every speed has its own setup and is customizable according to user demand. Figure 8 shows the GPS arrangement inside the experimental vehicle.

Figure 7: MINITAUR Box (GPS) (DEWESoft, n.d.)

Figure 8: Arrangement of GPS inside the experimental vehicle

The GPS also comes with an antenna attached on top of the vehicle for better signal reception. The antenna is used to receive GPS signal from satellite to the experimental vehicle. The GPS receiver is attached as shown in Figure 9.

Figure 9: GPS receiver (antenna)

Next, the WSS used in this study is known as the incremental rotary encoder (e.g., Sendix 5020 with hollow shaft) as depicted in Figure 10. It offers high resistance against vibration and installation errors. Furthermore, its rugged housing has high protection level of up to IP67, as well as wide temperature range of -40°C up to +85°C, which makes this product the perfect encoder for all applications, especially for localization purpose. Table 1 shows the device mechanical characteristics.

Figure 10: Wheel speed sensor, incremental encoder type (Kuebler Technology News, 2016)

Table 1: Mechanical characteristics of the incremental rotary encoder

Characteristics	Type	Descriptions
1. Max speed	IP65	12,000 min^{-1}
		6,000 min-1 (continuous)
	IP67	6,000 min^{-1}
		3,000 min^{-1} (continuous)
2. Moment of inertia	Shaft version	Approx. 1.8 x 10^{-6} kgm^2
	Hollow shaft version	Approx. 6 x 10^{-6} kgm^2
3. Starting torque	IP65	< 0.01 Nm
	IP67	< 0.05 Nm
4. Shaft load capacity	Radial	80 N
	Axial	40 N
5. Working temperature range		-40°C up to +85°C
6. Material	Shaft	Stainless Steel
7. Shock resistance		2500 m/s^2, 6 ms
8. Vibration resistance		100 m/s^2, 10 ... 2,000 Hz

The incremental encoders generate an output signal each time the shaft rotates by a certain amount. When the power is switched on, the encoder starts counting from zero notwithstanding the position of the shaft. It is inevitable for the initial homing to a reference point to happen in all positioning tasks and both happen upon the start-up of the control system. Moreover, by using the rotation of the encoder (revolution per minute), Equation 6 is needed to transform the RPM in the form of km per hour (km/h) by considering the diameter of the vehicle wheel in meter (m).

$$velocity\ \left(\frac{km}{h}\right) = 2 * \pi * 0.55 * \left(\frac{60}{1000}\right) \quad (6)$$

where the diameter of the wheel is 55 cm or 0.55 meter.

Last but not least is the installation of the IMU. The IMU used in this study is MTi-100, a product from Xsens, as shown in Figure 11. The IMU can provide three main data, namely the vehicle's roll, pitch and yaw. However, only yaw rate data are collected from the IMU for the purpose of this research.

According to its specifications, the IMU can either be gimballed-type or strap-down, outputting the integrating quantities of angular velocity and acceleration in the sensor/body

frame. IMUs are commonly explained in literature as the rate-integrating gyroscopes and accelerometers. The MTi 100- series has an input voltage up to 34 V and its typical power consumption is 675 – 950 mW. Furthermore, it has 10 kHz sampling frequency per channel and generates up to 2 kHz of output frequency. Moreover, the IMU has a standard full range gyro of 450 °/s and a standard full range acceleration of 50 m/s^2. All these specifications are very important in generating good yaw rate data from the vehicle.

Figure 11: MTi-100 IMU (Xsens, n.d.)

2.2 DEWESoft Software

Once the installation part is complete, understanding of DEWESoft software is required. DEWESoft is a data acquisition software package allowing the user to display and record data from A/D boards, and to control signal conditioners. It is easy to use and can synchronise data acquisition of different sources. Furthermore, it can export data to almost any analysis package and has powerful online mathematics and filtering. Via the software, all data from the WSS, IMU and GPS can be recorded simultaneously. Figure 12 shows a viewer part of the DEWESoft software.

Figure 12: DEWESoft software

2.3 Research Design

This step comprises the integration of hardware (i.e., the WSS and IMU) and MATLAB software, data collection and conversion into X and Y coordinates. The purpose of integrating both the hardware and MATLAB is to design a model-based simulation system to extract and simulate the collected data and compare them with the actual data from the hardware. This step includes comparing the operations between the velocity data generated by the vehicle's ECU and velocity data by the WSS. The result will be shown in the next chapter.

In MATLAB, there are two main systems created called the Path System (Figure 13) and Yaw System, (Figure 14). Path System is used for generating the localization path while Yaw System is used for analysis process.

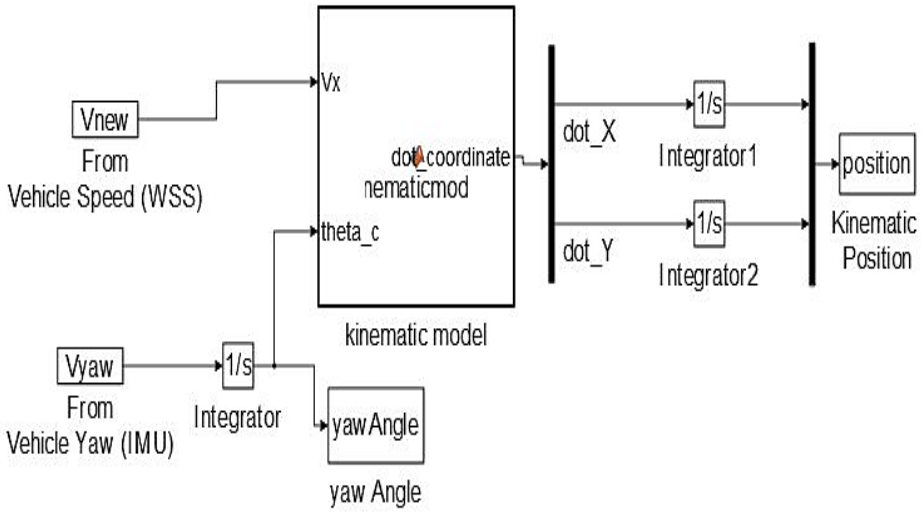

Figure 13: Path System

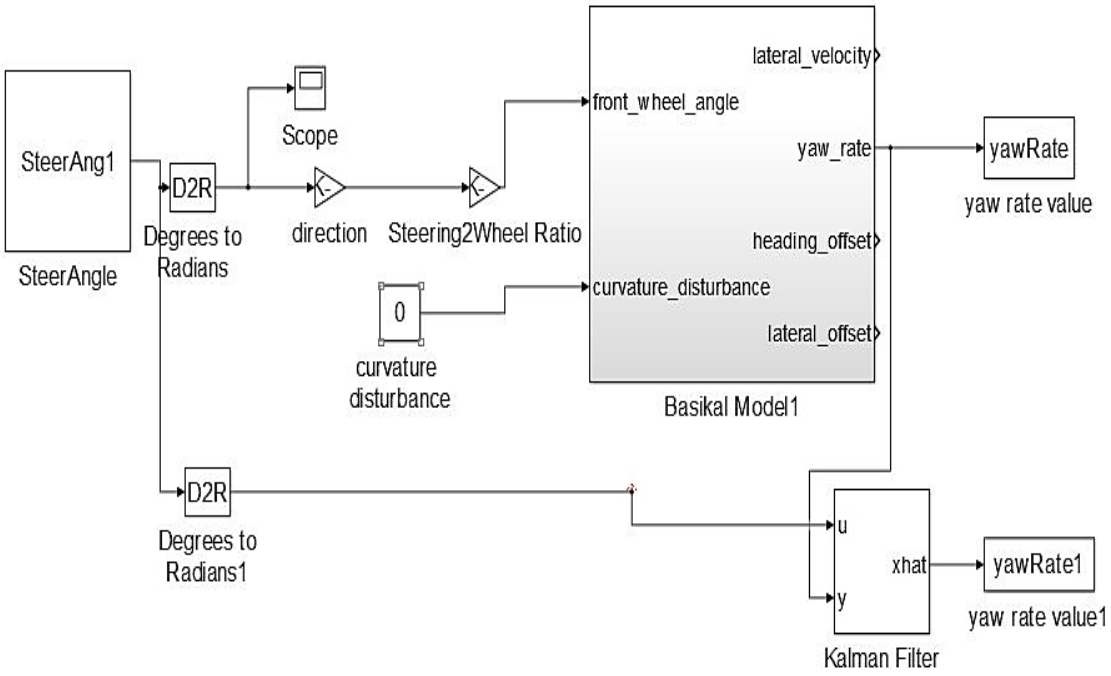

Figure 14: Yaw System

In the Path System, velocity captured from WSS and yaw rate data from IMU will be used as inputs. Both the data will be combined through Kinematic Modelling and be integrated in order to get the global position (X and Y coordinates). All data were processed with the same sampling time of 1 millisecond for synchronization. The following equations represent the kinematic model:

$$X\_coor = velocity * \cos(yaw\ rate) \quad (7)$$

$$Y\_coor = velocity * \sin(yaw\ rate) \quad (8)$$

While in Yaw System, a bicycle model is applied to generate yaw rate of the vehicle i.e., instead of using the raw yaw rate from IMU based on the steering angle, it will be collected from the vehicle ECU as the input. The purpose of using the bicycle model is to support the yaw rate data collected from the IMU. Thus, the localization path generated from the combination of yaw rate and velocity is true.

In addition, the Kalman Filter or estimator in Path system is implemented to fuse the yaw rate data produced from the bicycle model with the vehicle steering angle. The purpose of the estimator is to produce a predicted yaw rate by adding noise or interference to the system to resemble actual occurrence of the vehicle with reference to the steering angle of a real driving condition.

3.0 RESULTS AND DISCUSSION

3.1 Comparison between Velocity from WSS and ECU

As mentioned in Introduction section, velocity from the ECU is generated by rotation of the crankshaft inside the engine per minute while velocity from the WSS is generated by the rotation of the vehicle wheel per minute. It is clear that the ECU uses an internal sensor (crankshaft) to generate velocity while the WSS is an external sensor. In order to determine which sensor is effective, both velocity data are compared in the same plan. Figure 15 shows the comparison between the velocity from ECU and WSS.

There was only a slight difference between both velocities. The velocity from the WSS was smaller compared to that of the ECU. This occurred due to the existence of frictional force between the wheel and road surface. As mentioned before, the WSS is an external sensor, and is more practical as it includes the frictional force into the calculation to generate velocity. The difference between both velocities shows the amount of frictional force which exists at that particular time.

Furthermore, the WSS sensor generated a high number of sampling data. Clearly, there are a lot of blue colour data rather than orange colour data. This is due to the effects from the higher number of data sampling. Therefore, in terms of smooth data, velocity from the ECU is smoother than that of WSS due to the latter being an external sensor, and may be effected by environmental noise.

However, in terms of velocity accuracy, WSS generated much better accuracy compared to ECU. In order to perform the localization operation, a high accuracy of velocity data is needed. Otherwise, the system will be unable to detect a vehicle's exact position from time to time. This situation is crucial when it comes to autonomous operation.

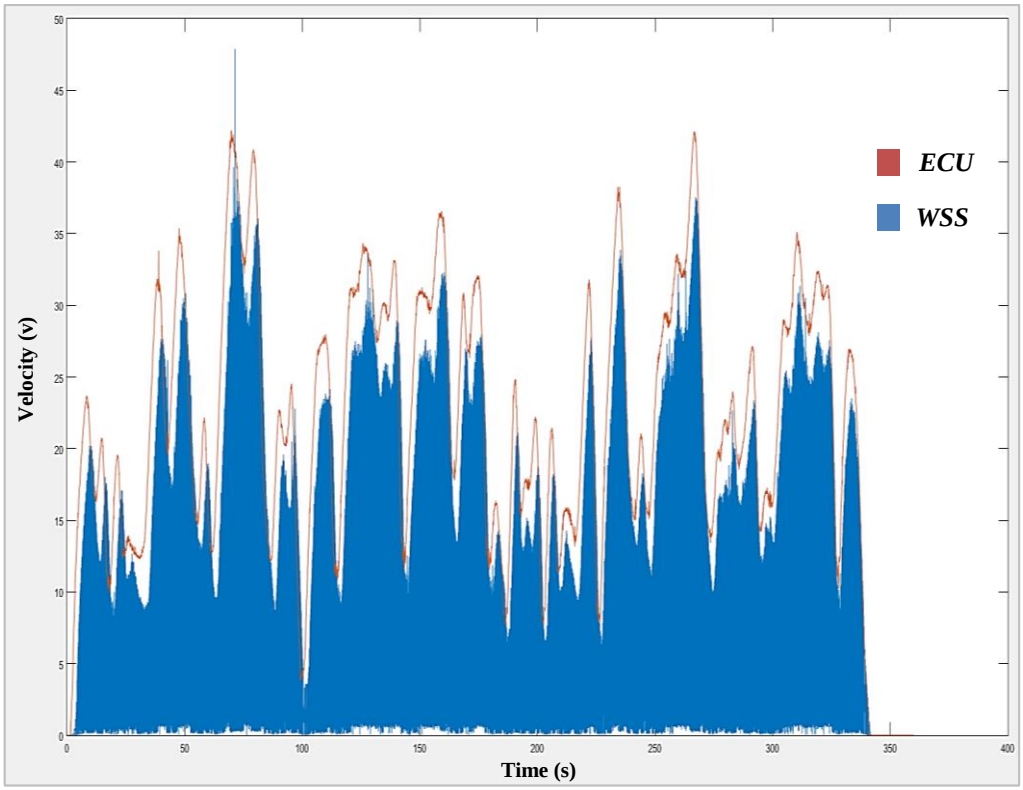

Figure 15: Comparison between velocity collected from Engine Control Unit (ECU) and velocity collected from Wheel Speed Sensor (WSS)

3.2 Comparison between Raw Yaw Rate from IMU and Estimated Yaw Rate from Bicycle Model

As mentioned earlier, the purpose of this analysis is to validate the raw yaw rate from the IMU using the estimated yaw rate from the Bicycle Model. Therefore, the localization path to be generated from the raw yaw rate is regarded as trusted and acceptable. Figure 16 shows the comparison between raw yaw rate and the estimated yaw rate.

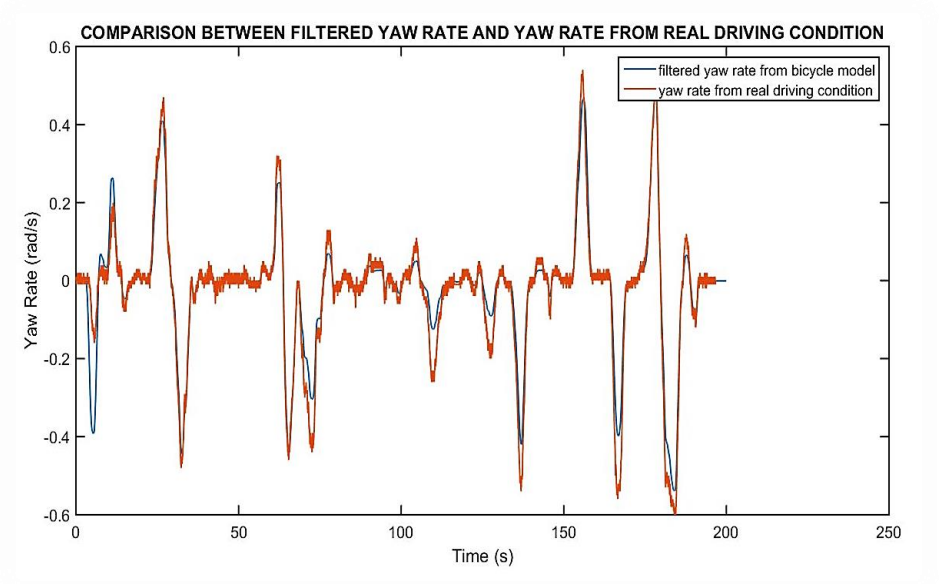

Figure 16: Comparison between filtered yaw rate from the bicycle model and yaw rate from the IMU

Both yaw rate are almost identical. However, as observed in the first 10 seconds of the data collection, the estimated yaw rate experience high value of yaw rate compared to the raw yaw rate. The difference is quite huge. This is due to the fusion operation between the steering angle and the pure yaw rate through Kalman Filter.

The pattern of steering angle data is different in the first 10 seconds of data collection as opposed to raw yaw rate, as shown in Figure 17.

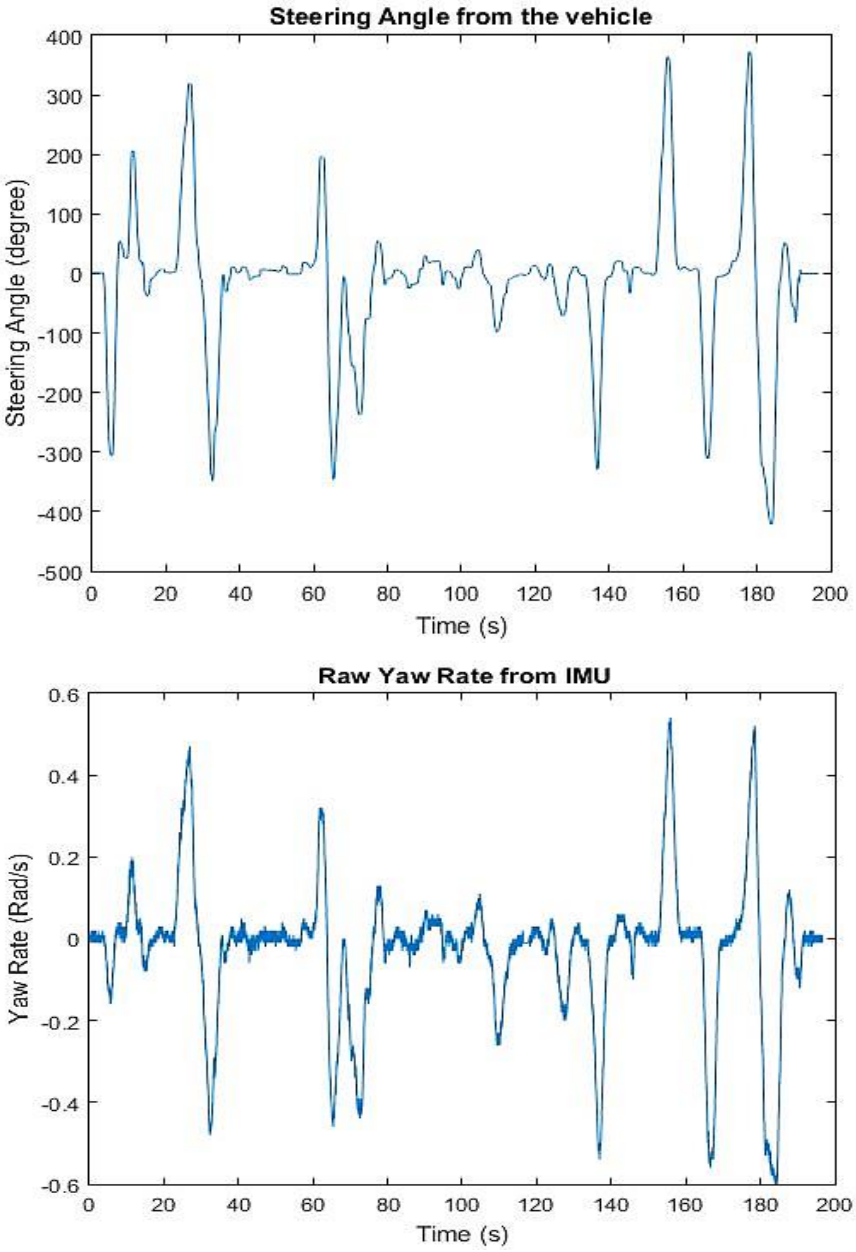

Figure 17: Comparison between pattern of raw steering angle and raw yaw rate from vehicle

This is probably due to some technical issues of the WSS or the vehicle itself that occurred during the first 10 seconds of data collection. However, the total data has more than 85% similarity. Therefore, the data are considered acceptable.

3.3 Comparison between Localization Path from WSS and IMU with Localization Path from GPS

After velocity from WSS and yaw rate from IMU were analysed, both data will be combined through Kinematic Modelling as discussed earlier to generate the localization path result. Later, the result will be compared with the localization path generated from GPS.

Unfortunately, both data had different type of scaling. The WSS and IMU only generated local position data (local coordinate) while GPS generated global position data (global coordinate). Therefore, both data cannot be compared in the same plane. The pattern difference of the localization path can be observed in Figure 18.

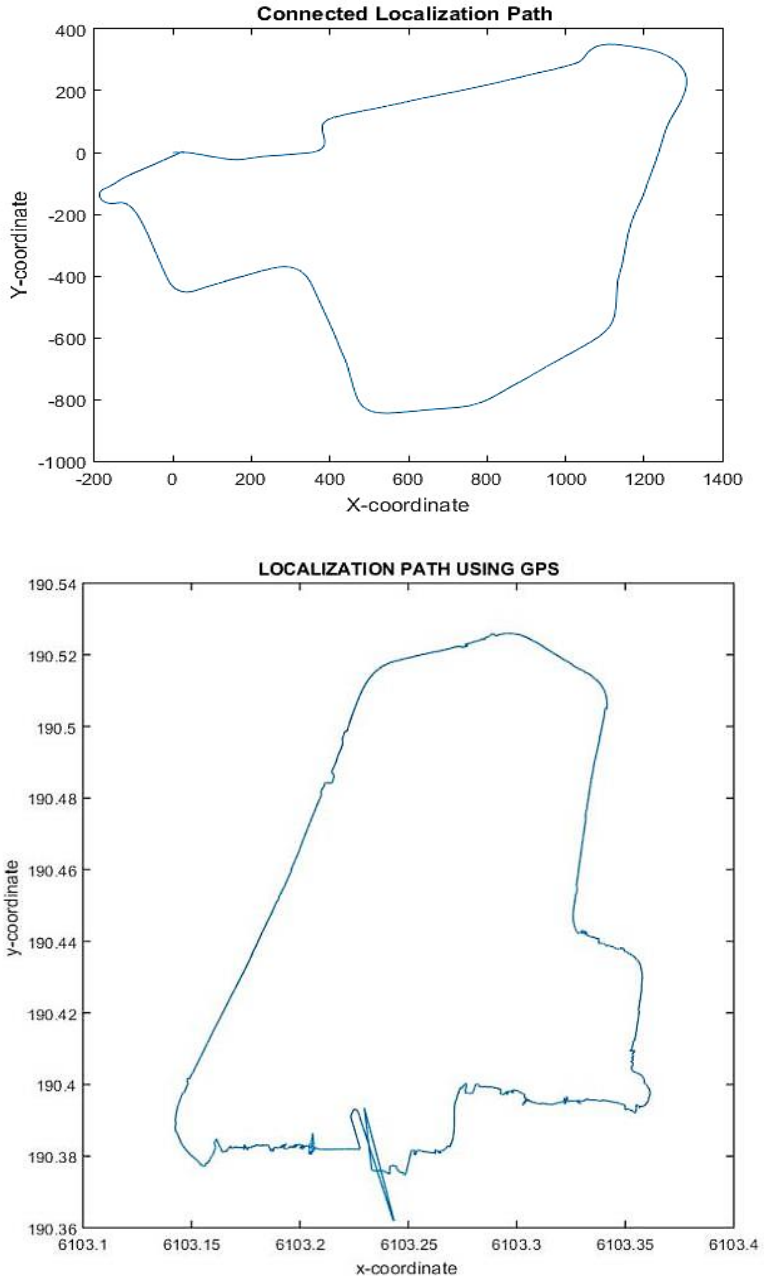

Figure 18: Pattern Comparison between Localization Path from WSS and IMU with GPS

In order to ascertain their similarity, the localization path from WSS and IMU is rotated by 180 degree. Hence, the similarity can be observed clearly. As mentioned before, the scale is different due to the local and global coordinates, see Figure 19.

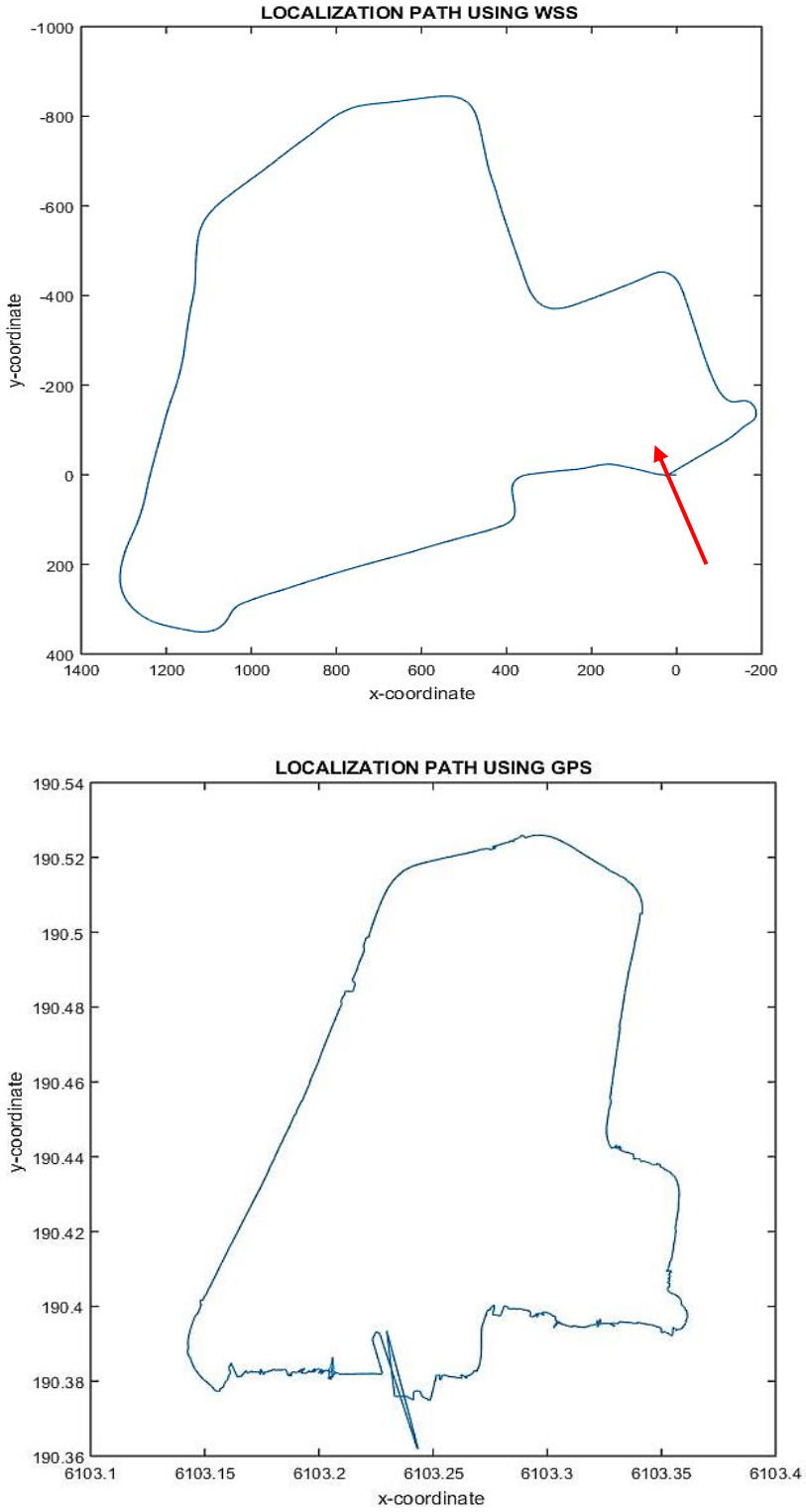

Figure 19: Pattern comparison between localization path from WSS and IMU with GPS after 180 rotations

By comparing both localization path side by side in Figure 19, it can be concluded that the velocity from WSS and the yaw rate from IMU managed to generate the same pattern as the localization path generated from the GPS. The only difference is seen at the red arrow section where a slight drifting still occurred. This was probably due to the limitation of WSS itself where it can only generate local position data, and not global position data.

3.4 Comparison with Google Map Localization Path

To determine the localization path generated in this research is correct, the localization path is compared with Google map as shown in Figure 20.

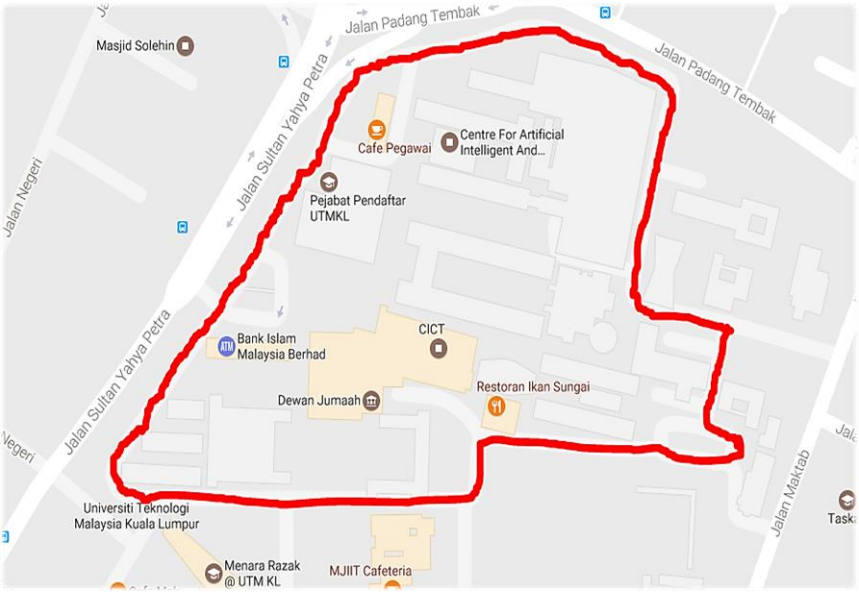

Figure 20: UTM KL Campus map taken from Google Map

The red line in the map was created by this author to show the path taken during data collection around UTM KL campus. By comparing the pattern with the localization path generated in Figure 19, it can be observed that the localization path generated is true.

4.0 CONCLUSION

The aim of this research is to determine whether WSS and IMU can distribute the same function as GPS in vehicle localization. The advantage of WSS and IMU for autonomous vehicle is that it can keep track of the vehicle's position even though it moves through tunnel or any GPS-denied area. Hence, by using the results obtained in subsection 3.3 and all of the yaw rate analyses in subsection 3.2, it is proved that WSS together with IMU can achieve the localization operation of a vehicle.

ACKNOWLEDGEMENTS

The work presented in this paper is supported by the Ministry of Education and Universiti Teknologi Malaysia under research university grant VOT 15H81.

REFERENCES

AerMech.com (2014). *ECU (engine control unit) cars, ECM, parts, functioning*. Retrieved from http://aermech.com/ecu-engine-control-unit-carsecmpartsfunctioning/

Axelrad, P., Comp, C.J., & Macdoran, P.F. (1996). SNR-based multipath error correction for GPS differential phase. *IEEE Transactions on Aerospace and Electronic Systems*, *32*(2), 650-660.

Belta, C., & Kumar, V. (2001). Motion generation for formation of robots: A geometric approach. *Proceedings of 2001 ICRA. IEEE International Conference on Robotics and Automation*, Seoul, South Korea.

DEWESoft (n.d.). MINITAURs - Compact all-in-one DAQ instrument. Trbovlje, Slovenia: DEWESoft d.o.o. Retrieved from https://www.dewesoft.com/products/minitaur-s

Kuebler Technology News (2016). *Incremental encoders feature robust design for use outdoors*. Charlotte, NC: Kuebler Group. Retrieved from http://www.kueblernews.com/

Marino, R., Scalzi, S., & Netto, M. (2012). Integrated driver and active steering control for vision-based lane keeping. *European Journal of Control*, *18*(5), 473-484.

Says.com (2015). 6 ways you could cause a traffic jam without even trying. Selangor, Malaysia: REV Social Malaysia Sdn. Bhd. Retrieved from http://says.com/my/fun/traffic-jams

Taheri, S. (1990). *An investigation and design of slip control braking systems integrated with four wheel steering* (PhD thesis). Clemson University, Clemson, South Carolina, US.

Tash, A. (2016). *Gridlock comes to Kuala Lumpur*. Retrieved from https://www.nytimes.com/2016/08/25/opinion/gridlock-comes-to-kuala-lumpur.html

The World Bank (2015). Annual report 2015. Washington, DC: The World Bank Group. Retrieved from http://www.worldbank.org/en/about/annual-report-2015/overview

Welch, G., & Bishop, G. (2006). An introduction to the Kalman filter. Department of Computer Science, University of North Carolina.

Xsens (n.d.). MTi 100-series. Enschede, Netherlands: Xsens Technologies B.V. Retrieved from https://www.xsens.com/products/mti-100-series/